JOURNAL OF MOLECULAR SPECTROSCOPY 151, 459–473 (1992)

Fourier Transform Jet Emission Spectroscopy of the $B^2\Sigma^+-X^2\Sigma^+$ Transition of CN

C. V. V. PRASAD AND P. F. BERNATH[1,2]

Centre for Molecular Beams and Laser Chemistry, Department of Chemistry, University of Waterloo, Waterloo, Ontario, Canada N2L 3G1

AND

C. FRUM AND R. ENGLEMAN, JR.[3]

Department of Chemistry, University of Arizona, Tucson, Arizona 85721

The violet ($B^2\Sigma^+-X^2\Sigma^+$) system of the CN molecule was produced in a jet-cooled, corona-excited, supersonic expansion of helium using methyl azide and diazoacetonitrile as precursor molecules. This spectrum was also excited in a Cossart source with a trace of methane in argon. The spectra were recorded with the McMath Fourier transform spectrometer of the National Solar Observatory. In the present work, the rotational structure of the 0–0 through 7–7 and 1–0 through 9–8 vibrational bands was analyzed.

INTRODUCTION

The CN free radical occurs in a wide variety of sources. In the laboratory, CN is abundant in flames and electrical discharges of all types, where it often forms from trace amounts of carbon and nitrogen. CN is also found in a wide variety of extraterrestrial sources including the Sun (*1*), stellar atmospheres (*2, 3*), comets (*4*), dark interstellar clouds (*5, 6*), and diffuse interstellar clouds (*7–12*) by the techniques of microwave, infrared, and ultraviolet spectroscopy.

Our interest in cold CN was sparked by discussions with J. Black on the observation of CN in absorption in diffuse interstellar clouds (*7–12*). The $B^2\Sigma^+-X^2\Sigma^+$ transition of CN is seen by absorption of the radiation of a bright star (for example, ζ Ophiuchi) by a diffuse interstellar cloud. The diffuse interstellar cloud lies in the path between the star and the Earth.

After the discovery of the 3 K cosmic background radiation (*13*), it was realized that the rotational energy level spacing of CN ($N = 1 \leftarrow 0$, $\lambda = 0.264$ cm, $\nu = 3.78$ cm^{-1} = 113 GHz = 5.4 K) is ideal for use as a cosmic thermometer (*14*). For example, the relative populations of the $N = 1$ and $N = 0$ levels of CN, as measured by optical absorption, give a temperature of 2.83 ± 0.09 K (*12*) in good agreement with value of 2.3 K derived by McKellar in 1941 (*15*). McKellar (*16*) was the first to identify the lines of the CN violet system observed in diffuse interstellar clouds by Adams and other astronomers (*17*).

[1] Also Department of Chemistry, University of Arizona, Tucson, AZ 85721.

[2] Camille and Henry Dreyfus Teacher–Scholar.

[3] Current address: Department of Chemistry, University of New Mexico, Albuquerque, NM 87131.

0022-2852/92 $3.00

The CN molecule has been the subject of numerous laboratory investigations. The first rotational analyses of the $B^2\Sigma^+$–$X^2\Sigma^+$ violet system was by Kratzer (*18*) and by Jevons (*19*), although efforts to assign the carrier and to understand the rovibrational structure were made more than a century ago. Jenkins (*20*) extended the analysis to the "tail" bands of the violet system. More recent analyses are given by Engleman (*21*) and by Schoonveld and Sundaram (*22*). For a detailed review of the literature, the reader is referred to the articles by Douglas and Routly (*23*) and Brocklehurst *et al.* (*24*) and the book by Huber and Herzberg (*25*).

More recent work includes the observation of microwave and millimeter-wave transitions in the $X^2\Sigma^+$ state for $v = 0$ and 1 (*26*), for $v = 0$–3 (*27*), for $v = 2$ (*28*), and for $v = 3$–10 (*29*). These data are particularly useful in our analysis of the $B^2\Sigma^+$–$X^2\Sigma^+$ transition because they help break the correlations between the B and X state constants. The corresponding data for $v = 0$ of the $X^2\Sigma^+$ state of ^{13}CN were measured by Bogey *et al.* (*30*).

The $B^2\Sigma^+$ state displays the effects of many perturbations due to interactions with the $A^2\Pi_i$ and $X^2\Sigma^+$ states as well as two quartet states. The perturbations of CN have been studied extensively by, most notably, Kotlar *et al.* (*31*) and Ito, Kuchitsu, and co-workers (*32–36*). Other recent work includes the observation of the vibration–rotation spectrum by Fourier transform spectroscopy (*37*) as well as ab initio and experimental determinations of the $B^2\Sigma^+$–$X^2\Sigma^+$ transition dipole moment function (*38–41*).

Our work on cold CN began several years ago when strong emission from the $B^2\Sigma^+$–$X^2\Sigma^+$ violet system was found in supersonic jet spectra of the free radicals CH_3N (*42*) and CCN (*43*). A corona-excited supersonic jet expansion (*44*) of methyl

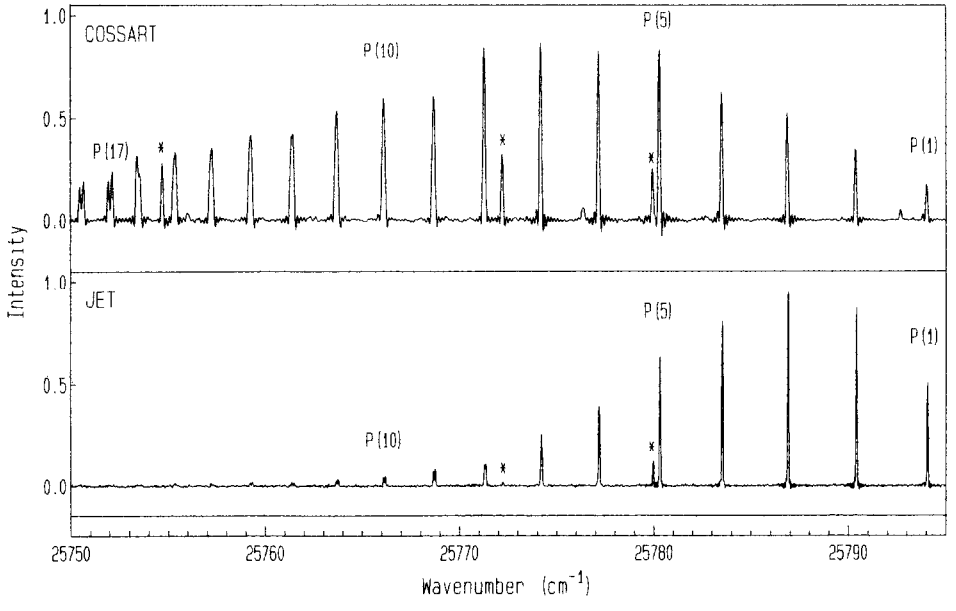

FIG. 1. Part of the P branch of the 0–0 band of the violet system of the CN molecule produced in the Cossart and jet sources. The spectral lines marked with an asterisk are the extra lines occurring in the spectrum because of the perturbations in the $v = 0$ level of the $B^2\Sigma^+$ state.

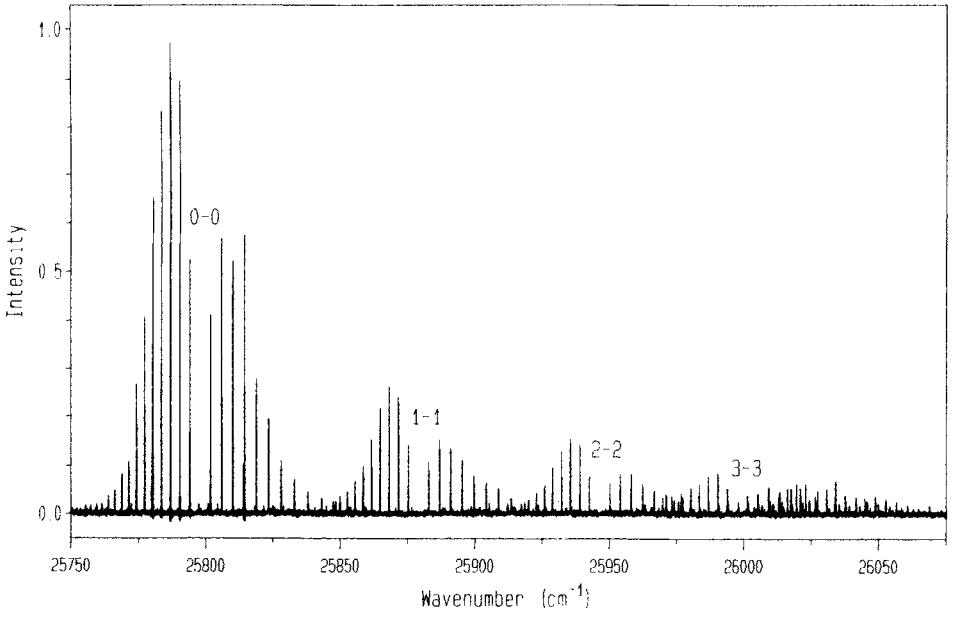

FIG. 2. The $\Delta v = 0$ sequence of the B–X system of the CN molecule produced in the jet source with methyl azide as a precursor molecule. The 3–3 through 7–7 bands are overlapped.

azide and diazoacetonitrile precursors in He provided rotational cold (30 K) emission spectra. In addition, a room temperature emission spectrum of the violet system was available from a Cossart discharge lamp. In this spectrum CN appeared (as usual) as

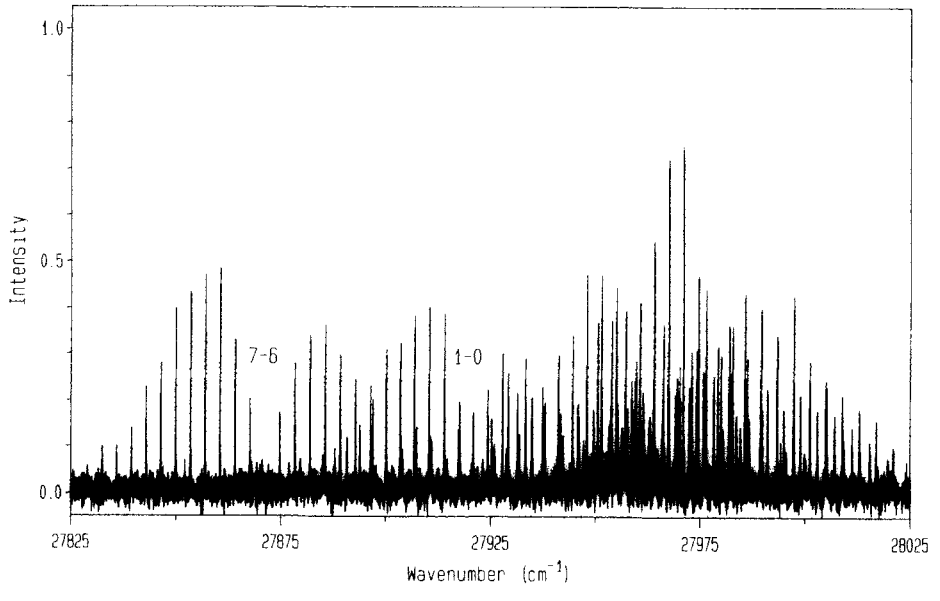

FIG. 3. The $\Delta v = +1$ sequence of the B–X system of the CN molecule produced in the jet source with diazoacetonitrile as precursor molecule. The 2–1 through 6–5 bands are overlapped while the 8–7 and 9–8 bands lie below 27 825 cm^{-1}.

TABLE I

Vacuum Wavenumbers (in cm^{-1}) for the Rotational Lines of the Bands of the Violet ($B^2\Sigma^+ - X^2\Sigma^+$) System of the CN Molecule

N	$R_1(N)$	$R_2(N)$	$P_1(N)$	$P_2(N)$
		0-0 BAND[a]		
0	25801.787(-8)			
1	25805.854(1)	25805.821(1)	25794.088(4)	
2	25810.039(-6)	25809.997(-7)	25790.444(3)	25790.435(0)
3	25814.354(-18)	25814.382(62)	25786.935(0)	25786.918(0)
4	25818.826(-8)	25818.774(2)	25783.561(-4)	25783.535(-2)
5	25823.411(-19)	25823.355(-3)	25780.323(-8)	25780.345(52)
6	25828.023(-137)	25828.083(4)	25777.224(-7)	25777.187(3)
7	25833.047(22)	25832.937(3)	25774.254(-15)	25774.215(3)
8	25838.030(7)	25837.928(7)	25771.308(-134)	25771.382(6)
9	25843.160(5)	25843.050(6)	25768.772(20)	25768.677(1)
10	25848.420(-1)	25848.285(-15)	25766.208(9)	25766.115(3)
11	25853.812(-7)	25853.689(1)	25763.786(4)	25763.686(1)
12	25859.339(-12)	25859.206(-4)	25761.505(4)	25761.391(-5)
13	25864.992(-23)	25864.844(-21)	25759.367(9)	25759.253(11)
14	25870.656(-157)	25870.530(-122)	25757.331(-20)	25757.222(-3)
15	25876.775(32)	25876.570(-2)	25755.462(-20)	25755.348(1)
16	25882.836(31)	25882.624(-1)	25753.612(-138)	25753.467(-137)
17	25889.013(14)	25888.807(-1)	25752.187(32)	25751.996(-3)
18	25895.318(-6)	25895.117(-8)	25750.713(16)	25750.527(-5)
19	25901.792(10)	25901.577(6)	25749.387(10)	25749.196(-5)
20	25908.371(1)	25908.156(6)	25748.200(6)	25748.005(-4)
21	25915.086(-4)	25914.854(-6)	25747.151(2)	25746.950(-4)
22	25921.936(-4)	25921.703(2)	25746.241(0)	25746.036(0)
23	-	-	25745.471(-1)	25745.261(4)
25	25943.261(-13)	25943.018(12)		
		1-1 BAND		
0	25882.922(-10)			
1	25886.929(4)		25875.300(4)	
2	25891.060(3)		25871.681(3)	
3	25895.346(-1)	25895.284(-5)	25868.191(3)	
4	25899.738(-3)	25899.667(-6)	25864.831(3)	
5	25904.260(-3)	25904.180(-4)	25861.599(2)	
6	25908.914(0)	25908.814(-9)	25858.499(4)	
7	25913.690(-1)	25913.584(-5)	25855.549(-6)	25855.483(-8)
8	25918.602(7)	25918.478(-5)	25852.719(1)	25852.642(0)
9	25923.635(9)	25923.490(-13)	25850.010(-1)	25849.915(-9)
10	25928.788(3)	25928.674(24)	25847.442(8)	25847.336(1)
11	-	-	25844.987(1)	25844.882(6)
		2-2 BAND		
0	25950.190(-1)			
1	25954.148(14)		25942.647(15)	
2	25958.220(11)		25939.056(14)	
3	25962.441(10)	25962.381(2)	25935.584(11)	
4	25966.764(12)	25966.674(-16)	25932.233(9)	
5	25971.208(14)	25971.107(-15)	25929.008(10)	
6	25975.750(-7)	25975.657(-18)	25925.923(5)	25925.865(-5)
7	25980.435(-5)	25980.357(8)	25922.937(-4)	25922.868(-15)
8	-	-	25920.085(-1)	25920.004(-14)
9	-	-	25917.353(-2)	25917.257(-21)
10	-	-	25914.700(-48)	25914.620(-39)
11	-	-	25912.259(-5)	25912.122(-44)

[a] The spectral lines with wavenumbers 25 754.726, 25 772.234, 25 779.956, 25 813.983, 25 828.951, and 25 871.790 cm^{-1} are identified as the extra lines in the 0–0 band due to perturbations in the $v = 0$ level of the $B^2\Sigma^+$ state. One line belonging to the satellite branch ${}^RQ_{21}(0)$ is also observed at 25 801.769(−1) cm^{-1}.

TABLE I—*Continued*

N	$R_1(N)$	$R_2(N)$	$P_1(N)$	$P_2(N)$
		3-3 BAND		
0	26001.392(-9)			
1	26005.297(13)		25993.926(6)	
2	26009.331(4)	26009.265(4)	25990.361(7)	
3	26013.457(2)	26013.369(-3)	25986.906(7)	
4	26017.703(8)	26017.589(-6)	25983.574(19)	
5	26022.046(2)	26021.928(1)	25980.357(-1)	25980.286(-2)
6	26026.500(-4)	26026.370(1)	25977.257(10)	25977.163(3)
7	26031.074(0)	26030.916(-6)	25974.245(-1)	25974.142(-2)
8	-	-	25971.358(-1)	25971.208(-31)
		4-4 BAND		
0	26033.942(-22)			
1	26037.792(2)		26026.571(3)	
2	26041.728(2)		26023.020(-4)	
3	26045.783(-13)	26045.718(-6)	26019.576(-4)	
4	26049.935(1)	26049.847(0)	26016.232(-1)	
5	26054.172(5)	26054.069(4)	26012.994(8)	
6	-	-	26009.874(1)	26009.798(-1)
7	-	-	26006.825(-3)	26006.738(0)
8	-	-	26003.892(15)	26003.790(15)
		5-5 BAND		
0	26044.994(-32)			
1	26048.838(5)	26048.764(-9)	26037.661(-38)	
2	26052.752(21)	26052.645(-5)	26034.171(-16)	
3	26056.707(-7)	26056.612(0)	26030.796(3)	26030.738(-9)
4	26060.736(-39)	26060.654(3)	26027.495(16)	26027.419(8)
5	-	-	26024.248(-2)	26024.163(1)
		6-6 BAND		
1	26035.449(-18)	26035.370(-47)	26024.529(-1)	
2	26039.244(-3)	26039.175(-3)	26021.025(1)	
3	26043.094(2)	26043.008(1)	26017.589(3)	
4	26047.012(7)	26046.902(0)	26014.243(1)	26014.181(-7)
5	-	-	26010.955(7)	26010.861(-15)
6	-	-	26007.730(8)	26007.624(-9)
7	-	-	26004.563(-2)	26004.469(10)
		7-7 BAND		
0	25990.754(7)			
1	25994.373(6)		-	
2	25998.040(-1)		25980.137(5)	
3	26001.756(-5)		25976.690(0)	
4	26005.515(-8)		25973.297(4)	
5	-		25969.936(-8)	
8	-		25960.140(-26)	
		1-0 BAND		
0	27925.331(-8)			
1	27929.287(-9)		27917.665(-3)	
2	27933.357(-2)		27913.977(-3)	
3	27937.514(-2)		27910.381(-5)	
4	27941.797(32)		27906.886(-1)	
5	27946.103(-5)		27903.477(-4)	
6	27950.601(58)		27900.147(-24)	
7	27955.055(-16)		27896.968(-18)	27896.885(-38)
8	27959.750(59)		27893.877(6)	27893.811(16)

TABLE I—*Continued*

N	$R_1(N)$	$R_2(N)$	$P_1(N)$	$P_2(N)$
		1-0 BAND		
9	27964.467(63)		27890.852(3)	27890.742(-22)
10	27969.275(68)		27887.956(33)	27887.803(-23)
11	27974.210(34)	27974.047(15)	27885.073(-19)	27884.925(-59)
12	27979.269(100)	27979.045(32)	27882.353(-3)	27882.228(-9)
13	27984.224(-29)	27984.088(3)	27879.736(21)	27879.591(6)
14	27989.428(1)	27989.235(-14)	27877.178(8)	27877.026(-2)
15	27994.697(5)	27994.490(-13)	27874.744(25)	27874.594(27)
16	28000.056(8)	27999.898(51)	27872.371(6)	27872.218(17)
17	28005.437(-56)	28005.226(-57)	27870.097(-8)	27869.943(13)
18	-	-	27867.948(8)	27867.755(0)
19	-	-	27865.886(15)	27865.689(14)
20	-	-	27863.883(-15)	27863.732(41)
21	-	-	27862.026(6)	27861.856(54)
22	-	-	27860.272(34)	27860.047(39)
		2-1 BAND		
0	27966.294(-14)			
1	27970.212(-4)		27958.712(-3)	
2	27974.219(-3)		27955.055(0)	
3	27978.343(30)		27951.476(-5)	
4	27982.504(15)		27947.990(-2)	
5	27986.743(-9)		27944.583(-8)	
6	27991.152(52)		27941.285(8)	
7	27995.616(37)	27995.555(67)	27938.075(-4)	27938.008(-14)
8	28000.105(1)	28000.027(25)	-	-
		3-2 BAND		
0	27991.152(-24)			
1	27995.014(-9)		27983.639(-20)	
2	27998.959(-3)		27980.022(0)	
3	28003.022(3)	28002.937(1)	27976.462(0)	
4	28007.115(-3)	28007.012(-6)	27972.985(6)	
5	28011.286(-6)	28011.180(5)	27969.612(7)	27969.527(-10)
6	28015.580(39)	28015.424(17)	27966.294(10)	27966.201(3)
7	28019.901(36)	28019.746(32)	27963.034(-4)	27962.915(-21)
8	28024.264(0)	28024.150(54)	27959.874(4)	27959.750(0)
9	-	-	27956.782(2)	27956.641(-2)
10	-	-	27953.748(-19)	27953.618(5)
		4-3 BAND		
0	27997.355(-1)			
1	28001.144(-2)		27989.927(3)	
2	28005.003(-9)		27986.313(3)	
3	28008.948(7)		27982.765(4)	
4	28012.879(-52)		27979.278(4)	
5	28016.974(-6)		27975.862(12)	
6	28021.084(-5)		27972.458(-31)	
7	28025.256(2)		27969.195(5)	
8	-		27965.940(-11)	
9	-		27962.769(-2)	
		5-4 BAND		
0	27981.967(-8)			
1	27985.761(44)		27974.602(-11)	
2	27989.526(-8)		27971.044(14)	

TABLE I—*Continued*

N	$R_1(N)$	$R_2(N)$	$P_1(N)$	$P_2(N)$
		5-4 BAND		
3	27993.384(-16)		27967.551(43)	
4	27997.284(-25)		27964.049(7)	
5	28001.252(1)		27960.620(-6)	
		6-5 BAND		
0	27942.272(-8)			
1	27945.938(5)		27935.013(-8)	
2	27949.630(-2)		27931.441(-3)	
3	27953.401(37)		27927.900(0)	
4	27957.064(-62)		27924.418(31)	
5	27960.986(66)		27920.920(12)	
6	27964.802(-12)	27964.694(16)	27917.502(-2)	27917.414(-2)
7	-	-	27914.109(10)	27913.977(-16)
8	27972.540(-41)	27972.458(47)	27910.723(-4)	27910.618(13)
9	27976.462(-53)	27976.330(3)	27907.402(12)	27907.248(-3)
10	27980.482(-1)	27980.281(3)	27904.076(-14)	27903.918(-15)
		7-6 BAND		
0	27874.768(-2)			
1	27878.360(3)		27867.614(6)	
2	27881.961(1)		27864.053(3)	
3	27885.571(-1)		27860.501(0)	
4	27889.190(-3)		27856.962(0)	
5	27892.821(0)		27853.433(-1)	
6	27896.451(-6)		27849.915(-2)	
7	27900.147(49)		27846.399(-9)	
8	27903.721(-23)		27842.904(-5)	
9	27907.402(11)		27839.410(-8)	
10	27911.048(7)		27835.933(0)	
11	27914.686(-3)		27832.533(58)	27832.447(15)
12	-		27829.025(21)	27828.965(10)
13	-		27825.503(-5)	
14	-		27822.036(-2)	
15	-		27818.574(7)	
16	-		27815.093(-1)	
17	-		27811.629(12)	
18	-		27808.069(-63)	
19	-		27804.624(-14)	
		8-7 BAND		
0	27776.794(10)			
1	27780.295(20)		27769.672(-33)	
2	27783.773(-4)		27766.150(-5)	
3	27787.336(12)	27787.211(5)	27762.598(1)	
4	27790.821(9)	27790.679(8)	27759.015(-14)	
5	27794.311(23)	27794.101(-20)	27755.515(15)	27755.383(-13)
6	27797.769(19)	27797.537(-22)	27751.939(18)	27751.773(-20)
7	27801.210(13)	27800.955(-26)	27748.356(25)	27748.171(-6)
8	27804.624(-5)	27804.425(36)	27744.740(11)	27744.534(-17)
9	27808.069(23)	27807.771(-10)	27741.129(13)	27740.896(-16)
10	27811.486(41)	27811.123(-33)	27737.501(12)	27737.248(-13)
11	27814.830(2)	27814.518(4)	27733.842(-8)	27733.589(-9)
12	27818.185(-6)	27817.852(0)	27730.210(13)	27729.908(-13)
13	27821.528(-7)	27821.179(8)	27726.551(20)	27726.220(-10)
14	27824.830(-28)	27824.502(33)	27722.855(5)	27722.530(6)
15	27828.130(-29)	27827.779(33)	27719.154(0)	27718.816(13)
16	27831.421(-16)	27831.023(24)	27715.440(-2)	27715.068(3)
17	-	-	27711.709(-2)	27711.313(2)
18	-	-	27707.947(-16)	27707.546(7)

TABLE I—*Continued*

N	$R_1(N)+R_2(N)$	$P_1(N)+P_2(N)$
	9-8 BAND	
0	27645.566(13)	
1	27648.992(16)	27638.619(29)
2	27652.367(10)	27635.049(-6)
3	27655.709(10)	27631.481(5)
4	27658.983(-17)	27627.858(-2)
5	27662.264(5)	27624.198(-5)
6	27665.475(-1)	27620.509(2)
7	27668.653(3)	27616.757(-15)
8	27671.778(-3)	27612.985(-12)
9	27674.862(-6)	27609.180(-1)
10	27677.902(-6)	27605.326(1)
11	27680.883(-20)	27601.421(-5)
12	27683.862(13)	27597.479(-7)
13	27686.739(-7)	27593.501(-1)
14	27689.603(11)	27589.474(-1)
15	27692.326(-61)	27585.429(27)
16	27695.131(4)	27581.278(-5)
17	27697.880(68)	27577.137(20)
18	27700.393(-49)	27572.908(6)
19	27703.010(-1)	27568.630(-8)
20	27705.520(0)	27564.323(0)
21	-	27559.960(6)
22	-	27555.527(-5)
23	-	27551.042(-10)

an impurity during our efforts to record a spectrum of the $A^2\Delta$–$X^2\Pi$ transition of CH (*45*).

During the course of our work, an analysis of the 0–0 band of the $B^2\Sigma^+$–$X^2\Sigma^+$ transition recorded in a similar jet source appeared in the literature (*46*). In this work only the 0–0 band was analyzed and the Fourier transform spectra had only medium resolution (0.25 cm^{-1}). In our work we observed the 0–0 through 7–7 and the 1–0 through 9–8 vibrational bands of the violet system at 0.035 cm^{-1} resolution. Very recently, we learned of work very similar to our own by Rehfuss *et al.* at The Ohio State University (*47*). They recorded rotational cold spectra at high resolution in the $\Delta v = 0$ and $\Delta v = -1$ vibrational sequence bands up to $v = 13$.

EXPERIMENTAL DETAILS

The spectrum of the CN radical was produced in a corona-excited supersonic expansion (*44*). A potential of 3 kV was provided by a high voltage power supply through a ballast resistor of 2 MΩ to a 250-μm diameter tungsten wire. The tungsten wire ends 400 μm from a 250-μm diameter pinhole nozzle. Methyl azide (CH_3N_3) was used as the precursor molecule for the production of CN in the jet source and helium at a pressure of 2.3 atm was used as carrier gas (*42*). The pressure in the vacuum chamber was several hundred millitorr. The potential drop through the nozzle provided the electrical excitation to form a plasma. The subsequent expansion collisionally cooled the rotational motion of the molecules.

The electronic emission of the rotationally cooled molecules was observed by focusing the emission perpendicular to the molecular jet onto the entrance aperture of

TABLE II

Hyperfine-Free Transitions (in cm^{-1}) in the $X^2\Sigma^+$ State of the CN Molecule

	N′	J′	N″	J″	WAVENUMBER		N′	J′	N″	J″	WAVENUMBER
v=0						v=5					
	1	0.5	0	0.5	3.77490158(41)		1	0.5	0	0.5	3.60006229(4)
	1	1.5	0	0.5	3.78578334(-92)		1	1.5	0	0.5	3.61014358(66)
	2	1.5	1	1.5	7.54964617(-182)		2	1.5	1	0.5	7.21005063(12)
	2	1.5	1	0.5	7.56053001(-107)		2	2.5	1	1.5	7.21677048(-48)
	2	2.5	1	1.5	7.56778342(-305)						
	3	2.5	2	2.5	11.32408613(4)	v=6					
	3	2.5	2	1.5	11.34222273(-184)		1	0.5	0	0.5	3.56480134(-69)
	3	3.5	2	2.5	11.34947962(-34)		1	1.5	0	0.5	3.57461690(-75)
	4	3.5	3	2.5	15.12345981(483)		2	1.5	1	0.5	7.13926194(69)
							2	2.5	1	1.5	7.14580507(7)
v=1											
	1	0.5	0	0.5	3.74013418(98)	v=7					
	1	1.5	0	0.5	3.75089497(24)		1	0.5	0	0.5	3.52945672(-121)
	2	1.5	1	1.5	7.48011035(-116)		1	1.5	0	0.5	3.53892880(-155)
	2	1.5	1	0.5	7.49087386(82)		2	1.5	1	0.5	7.06822944(111)
	2	2.5	1	1.5	7.49804570(-170)		2	2.5	1	1.5	7.07454352(25)
	3	2.5	2	1.5	11.23771663(70)						
	3	3.5	2	2.5	11.24489060(32)	v=8					
							1	0.5	0	0.5	3.49404221(91)
v=2							1	1.5	0	0.5	3.50306009(2)
	1	0.5	0	0.5	3.70526585(-34)		2	1.5	1	1.5	6.99694565(-58)
	1	1.5	0	0.5	3.71589170(54)		2	2.5	1	1.5	7.00295874(-1)
	2	1.5	1	0.5	7.42100322(36)		3	2.5	2	1.5	10.49653407(-57)
	2	2.5	1	1.5	7.42808610(-8)		3	3.5	2	2.5	10.50254781(65)
	3	2.5	2	1.5	11.13288915(26)						
	3	3.5	2	2.5	11.13997166(-54)	v=9					
							1	1.5	0	0.5	3.46698248(-36)
v=3							3	2.5	2	1.5	10.38909644(-12)
	1	0.5	0	0.5	3.67029815(2)		3	3.5	2	2.5	10.39471061(24)
	1	1.5	0	0.5	3.68077094(11)						
	2	1.5	1	0.5	7.35091512(22)	v=10					
	2	2.5	1	1.5	7.35789667(-3)		3	2.5	2	1.5	10.28096641
	3	2.5	2	1.5	11.02773243(-21)		3	3.5	2	2.5	10.28619863
v=4											
	1	0.5	0	0.5	3.63522875(-58)						
	1	1.5	0	0.5	3.64552629(13)						
	2	1.5	1	0.5	7.28060014(77)						
	2	2.5	1	1.5	7.28746341(-52)						

the McMath Fourier transform spectrometer of the National Solar Observatory at Kitt Peak. A total of eight scans were recorded in 38 min of integration at a resolution of 0.035 cm^{-1}. A Corning color filter (CS 7-54) and two solar blind photomultiplier tube detectors limited the spectral range to 25 000–38 000 cm^{-1}.

The spectrum of CN was also produced in the same source using diazoacetonitrile (*43*) as the precursor molecule, with 5 kV of applied voltage and helium as a carrier gas at a pressure of 2.7 atm. A total of six scans were coadded in 28 min of integration at a resolution of 0.035 cm^{-1}. The spectrum recorded with methyl azide as a precursor was found to be good for the $\Delta v = 0$ sequence of the violet bands while the spectrum with diazoacetonitrile was found to be better for the $\Delta v = +1$ sequence.

The spectrum of CN was also produced in a Cossart source (*48*) with a trace of CH_4 in 2 Torr of argon gas on the low pressure side of the capillary discharge. The current was about 100 mA. Three scans were coadded in 22 min of integration at a

TABLE III

Molecular Constants (in cm^{-1}) for the $X^2\Sigma^+$ State of the CN Molecule

Vibrational level	T_v	B_v	D_v /10^{-6}	γ_v /10^{-3}
0	0.0	1.89109115(45)	6.432(19)	7.25539(88)
1	2042.4073(26)	1.87366668(73)	6.454(49)	7.1744(13)
2	4058.5250(42)	1.85618763(75)	6.437(50)	7.0833(20)
3	6048.2991(49)	1.83865280(77)	6.419(57)	6.9818(22)
4	8011.6909(59)	1.8210600(14)	6.50(20)	6.8646(23)
5	9948.6403(78)	1.8034042(14)	6.44(19)	6.7204(23)
6	11859.1670(84)	1.7856861(13)	6.60(18)	6.5437(23)
7	13743.1914(91)	1.76789977(98)	6.66(13)	6.3149(22)
8	---	1.75003983(52)[a]	6.464(34)[a]	6.0125(15)[a]
9	---	1.73210097(5)[b]	6.503[c]	5.61381(52)[b]
10	---	1.7140482[d]	6.545[e]	5.232[d]

[a] These parameters were obtained from a combined fit of the 9–8 band and the hyperfine-free frequencies of the $v = 8$ level of state X. The term value for the $v = 8$ level could not be estimated; instead the band origin of the 9–8 band was determined to be 27 642.0923(22) cm^{-1}.

[b] Estimated from three hyperfine-free wavenumbers of the $v = 9$ level.

[c] Fixed at a value obtained by fitting the hyperfine wavenumbers of the $v = 9$ level (Ito *et al.* (*29*)).

[d] Calculated from two hyperfine-free wavenumbers of the $v = 10$ level.

[e] Fixed at a value reported by Ito *et al.* (*29*).

resolution of 0.078 cm^{-1}. Two cooled photomultiplier detectors (RCA 31034) and $CuSO_4$ filters limited the spectral region to 18 000–29 000 cm^{-1}.

The rotational temperature in the Cossart source is relatively higher than in the jet source allowing the observation of transitions with higher N values. However, the spectral lines obtained from the jet source are narrower so the spin-splitting of the lines was observed for rotational levels lower than in the Cossart source. Parts of the P branch of the 0–0 band recorded in the jet and Cossart sources are compared in Fig. 1.

The spectra from the Cossart source were calibrated with the help of argon lines present in the spectrum using the line positions reported by Norlen (*49*). The spectra from the jet source were then calibrated (using CN itself) to put the jet source data on the same wavenumber scale as the Cossart source. The lines belonging to the 0–0, 1–0, and 7–6 bands were measured from the spectra collected from both the Cossart and the jet sources. The rotational lines with low N values were taken from the spectra recorded using the jet source, while those with high N were taken from those recorded using the Cossart source. The spectra of 8–7 and 9–8 bands were taken exclusively from the spectra of the Cossart source, while for the remaining bands the data collected from the jet source were used. The spectra produced in the jet source are shown at low dispersion for $\Delta v = 0$ and $+1$ sequences in Figs. 2 and 3, respectively.

The CN molecules in the jet source were found to have a non-Boltzmann rotational population distribution. At least two temperatures (32 and 97 K) were required to

TABLE IV

Molecular Constants (in cm^{-1}) for the $B^2\Sigma^+$ State of the CN Molecule

Vibrational level	T_v[a]	B_v	D_v /10^{-6}	γ_v /10^{-3}
0	25797.8694(17)	1.958713(18)	6.598(37)	17.14(14)
1	27921.4536(30)	1.938006(33)	6.752(86)	18.27(20)
2	30004.8735(40)	1.91670(17)	5.26(167)	17.07(64)
3	32045.9002(54)	1.89413(18)	6.12(210)	23.96(40)
4	34041.9038(57)	1.87042(23)	14.14(350)	21.56(78)
5	35989.9494(85)	1.85152(68)	79.1(158)	27.96(124)
6	37887.2709(85)	1.81893(13)	2.73(100)	23.94(48)
7	39730.3498(88)	1.791119(61)	12.81(34)	11.28(148)
8	41516.4354(97)	1.762255(54)	9.55(24)	30.97(24)
9	--	1.730432(28)[b]	10.106(67)[b]	--

[a] The term values listed here are relative to the $v = 0$ level of the $X^2\Sigma^+$ state.

[b] These parameters were obtained from a combined fit of the 9–8 band and the hyperfine-free frequencies of the $v = 8$ level of state X. The term value for $v = 9$ level could not be estimated, but the band origin of the 9–8 band was determined to be 27 642.0923(22) cm^{-1}.

TABLE V

Equilibrium Molecular Constants for the $X^2\Sigma^+$ and $B^2\Sigma^+$ States of CN

Molecular Constant	$X^2\Sigma^+$	$B^2\Sigma^+$ [a]
ω_e	2068.640(14)	-
$\omega_e x_e$	13.0988(82)	-
$\omega_e y_e$	-0.0113(17)	-
$\omega_e z_e$	0.00032(12)	-
$Y_{01}(B_e)$	1.8997807(23)	1.96882(14)
$-Y_{11}(\alpha_e)$	0.0173647(42)	0.02005(22)
$Y_{21}(\gamma_e)$	$-2.99(18)\times10^{-5}$	$-2.95(52)\times10^{-4}$
Y_{31}	$5.5(28)\times10^{-7}$	$2.48(34)\times10^{-5}$
Y_{41}	$-6.0(14)\times10^{-8}$	-
r_e(Å)	1.1718082(7)	1.15108(4)

Note. Constants are in inverse centimeters unless stated otherwise.

[a] A reasonable set of vibrational constants could not be obtained from the vibrational term values of the $B^2\Sigma^+$ state, probably due to the perturbations in this state.

TABLE VI

Predicted Low N Lines of the 1–0 and 0–0 Bands of the CN Violet System (in cm^{-1})

N	$R_1(N)$	$R_2(N)$	$^RQ_{21}(N)$	$P_1(N)$	$P_2(N)$	$^PQ_{12}(N)$
			0-0 BAND			
0	25801.795	--	25801.770	--	--	--
1	25805.853	25805.821	25805.810	25794.083	--	25794.094
2	25810.045	25810.004	25809.985	25790.441	25790.435	25790.460
			1-0 BAND			
0	27925.339	--	27925.311	--	--	--
1	27929.314	27929.279	27929.268	27917.668	--	27917.679
2	27933.382	27933.337	27933.318	27913.985	27913.976	27914.004

describe the rotational level populations of the $B^2\Sigma^+$ state under our experimental conditions. These two temperatures were derived by least-squares fitting of the integrated line intensities as a function of N using the usual formula (*50*). The observed translational temperature is 243 K calculated from the observed full width at half-maximum of 0.0565 cm^{-1}. The effective translational temperature is much higher than the rotational temperature because emission from an unmasked and unskimmed jet expansion from a pinhole was used.

ANALYSIS AND DISCUSSION

The violet system ($B^2\Sigma^+$–$X^2\Sigma^+$) of the CN molecule is a transition between two states which belong to Hund's case (b). The rotational structure of a band consists of four main branches, R_1, R_2, P_1, and P_2, and two satellite branches, $^RQ_{21}$ and $^PQ_{12}$ (*50*). The two satellite branches are normally very weak, and hence they are not observed in most cases. However, in the 0–0 band the $^RQ_{21}(0)$ line was found by fitting the blended $R(0) + {}^RQ_{21}(0)$ lines.

If the spin-splitting of the spectral lines is not resolved, one would see only one R branch and one P branch. In the present study, the spin-splitting was observed in all of the bands except the 7–7, 4–3, 5–4, and 9–8 bands. In the violet system, the bands with low v' and v'' are degraded to shorter wavelengths. However, because B'_v decreases faster than B''_v, as v increases, the bands with high v are degraded to longer wavelengths.

The data reduction program PC-DECOMP, developed by J. W. Brault at the National Solar Observatory, was used to measure the spectral lines. The rotational line profiles were fitted to Voigt lineshape functions. The strong lines show "ringing" caused by the $(\sin x/x)$ lineshape function of the Fourier transform spectrometer. The ringing was eliminated by using the "filter fitting" available in PC-DECOMP. The signal-to-noise ratio for very strong lines is about 100. The rotational quantum numbers and the vacuum wavenumbers of the lines of the 17 bands analyzed in this work are listed in Table I.

The PC-DECOMP program was used to fit the blended lines in an effort to extract improved line positions. For the 0–0 band, where the signal-to-noise ratio approaches

100 for the strongest lines, we tried to resolve badly blended lines with $N < 8$. These lines show no evidence of spin-splitting other than an increase in linewidth. Our fitting procedure is equivalent to Fourier deconvolution ("resolution enhancement"). We remain somewhat skeptical about the reliability of all such procedures but we report these fitted line positions in Table I.

The pure rotational transitions for $v = 0$–10 of the $X^2\Sigma^+$ state of CN were included in our analysis. The nuclear spin of nitrogen ($I = 1$) splits the rotational levels of CN into three hyperfine components ($F = J + 1$, J, $J - 1$) for $J > 1.5$. Since we wanted to include the microwave transitions (*26–29*) in our B–X fits (but we did not want to rewrite our fitting programs to include the effects of hyperfine structure), a two step procedure was used to obtain the pure rotational transitions free of the effects hyperfine structure.

For each v, the observed microwave and millimeter-wave transitions of CN were fitted alone to provide a set of rotational and hyperfine constants, which were then used to calculate a set of hyperfine corrections. The hyperfine corrections and the observed transitions (*27–29*) were combined to give a set of hyperfine-free pure rotational transitions. In our calculations for $v = 8$–10 the eQq_v values of Ito *et al.* (*29*) were used, while for $v = 10$, Ito's value for D_{10} was also used (*29*). The hyperfine-free transitions are provided in Table II and they were included directly in our B–X fits.

Initially, band-by-band fits were made using the data of Tables I and II. The usual effective Hamiltonian of Brown *et al.* (*51*) was used with matrix elements derived with Hund's case (a) basis functions. The energy level expressions based on these matrix elements are listed, for example, in a paper by Douay *et al.* (*52*).

For the final fit, all the data (except the lines of the 9–8 band) were combined in a simultaneous nonlinear least-squares fit with 67 parameters. In this fit, T_v, B_v, D_v, and γ_v were determined for the 17 different vibrational levels ($v = 0$–7 of the $X^2\Sigma^+$ state and $v = 0$–8 of the $B^2\Sigma^+$ state). These spectroscopic parameters are provided in Tables III and IV along with 1 SD uncertainty.

The 9–8 band does not connect with the other bands observed in our analysis so a separate fit was necessary. The line positions for this band (Table I) and the hyperfine-free pure rotational transitions for $v = 8$ of the $X^2\Sigma^+$ state (Table II) were fitted together to provide the constants reported in Table III for $v = 8$ of the X state and Table IV for $v = 9$ of the B state. In this band the spin-splitting was not resolved and hence γ_9 was set to zero. Tables I and II also report the observed-minus-calculated line positions in parentheses using the constants of Tables III and IV.

The B_v values of Tables III and IV were used in the usual polynomial expansions (*50*) in powers of $(v + \frac{1}{2})$ to obtain a set of equilibrium constants. These values are reported in Table V. In addition the vibrational term values were also reduced to a set of equilibrium vibrational constants for the $X^2\Sigma^+$ state. A reasonable fit could not be obtained for the $B^2\Sigma^+$ state presumably because of various perturbations to the vibrational structure.

The low temperature emission spectrum of the violet system of CN is ideal for the precise determination of line positions. In some sense the jet expansion technique provides experimental conditions which emulate the cold conditions where CN is found in interstellar space. In Table VI we report our best estimates for the line positions of the observed or potentially observable interstellar absorption lines. These line positions are calculated from our spectroscopic constants and should have an accuracy of better than ± 0.005 cm^{-1} for the lines of the 0–0 band and $\pm$ 0.01 cm^{-1} for those of the 1–0 band.

The jet source also complements the usual hot sources of CN such as electrical discharges and carbon arcs. These traditional sources provide data extending to much higher N values but the low N lines are almost always blended. The density of CN lines produced, for example, in the carbon-arc operated in air is very impressive. However, the relatively narrow linewidth and freedom from blending makes the jet source data a valuable addition to the extensive data sets produced by hot sources of CN.

ACKNOWLEDGMENTS

The National Solar Observatory is operated by the Association for Research in Astronomy, Inc., under contract with the National Science Foundation. We thank J. Wagner, C. Plymate, and G. Ladd for assistance in recording the spectra. We thank T. A. Miller and H. Ito for discussions and data prior to publication. We also thank R. W. Nicholls for providing Ref. (*24*). This work was supported by the NASA Origins of the Solar System Research Program and the Natural Sciences and Engineering Research Council of Canada (NSERC).

RECEIVED: August 21, 1991

REFERENCES

1. D. L. LAMBERT, *Mon. Not. R. Astron. Soc.* **138,** 143–179 (1968); C. SNEDEN AND D. L. LAMBERT, *Astrophys. J.* **259,** 381–391 (1982).
2. D. L. LAMBERT, J. A. BROWN, K. H. HINKLE, AND H. R. JOHNSON, *Astrophys. J.* **284,** 223–237 (1984).
3. A. WOOTTEN, S. M. LICHTEN, R. SAHAI, AND P. G. WANNIER, *Astrophys. J.* **257,** 151–160 (1982).
4. J. R. JOHNSON, U. FINK, AND H. P. LARSON, *Astrophys. J.* **270,** 769–777 (1983).
5. B. E. TURNER AND R. H. GAMMON, *Astrophys. J.* **198,** 71–89 (1975).
6. M. GERIN, F. COMBES, P. ENCRENAZ, R. LINKE, J. L. DESTOMBES, AND C. DEMUYNCK, *Astron. Astrophys.* **136,** L17–L20 (1984).
7. D. M. MEYER AND M. JURA, *Astrophys. J.* **276,** L1–L3 (1984); **297,** 119–132 (1985).
8. D. C. MORTON, *Astrophys. J.* **197,** 85–115 (1975).
9. D. L. LAMBERT, Y. SHEFFER, AND P. CRANE, *Astrophys. J.* **359,** L19–L22 (1990); S. R. FEDERMAN, A. C. DANKS, AND D. L. LAMBERT, *Astrophys. J.* **287,** 219–227 (1984).
10. P. CRANE, D. J. HEGYI, N. MANDOLESI, AND A. C. DANKS, *Astrophys. J.* **309,** 822–827 (1986).
11. J. H. BLACK AND E. F. VAN DISHOECK, *Astrophys. J.* **331,** 986–998 (1988).
12. D. M. MEYER, K. C. ROTH, AND I. HAWKINS, *Astrophys. J.* **343,** L1–L4 (1989).
13. A. A. PENZIAS, K. B. JEFFERTS, AND R. W. WILSON, *Phys. Rev. Lett.* **28,** 772–775 (1972).
14. P. THADDEUS, *Ann. Rev. Astron. Astrophys.* **10,** 305–334 (1972).
15. A. MCKELLAR, *Publ. Dom. Astrophys. Obs.* **7,** 251–272 (1941).
16. A. MCKELLAR, *Publ. Astron. Soc. Pac.* **52,** 187–192 (1940).
17. W. S. ADAMS, *Astrophys. J.* **93,** 11–23 (1941).
18. A. KRATZER, *Ann. Phys.* **71,** 72–103 (1923).
19. W. JEVONS, *Proc. R. Soc. London A* **112,** 407–441 (1926).
20. F. A. JENKINS, *Phys. Rev.* **31,** 539–558 (1928).
21. R. ENGLEMAN, JR., *J. Mol. Spectrosc.* **49,** 106–116 (1974).
22. L. SCHOONVELD AND S. SUNDARAM, *Astrophys. J. Suppl.* **41,** 669–674 (1979).
23. A. E. DOUGLAS AND P. M. ROUTLY, *Astrophys. J. Suppl.* **1,** 295–318 (1955).
24. B. BROCKLEHURST, G. R. HÉBERT, S. H. INNANEN, R. M. SEEL, AND R. W. NICHOLLS, "Identification Atlas of Molecular Spectra, Vol. 9, The CN $B^2\Sigma^+$–$X^2\Sigma^+$ Violet System," Centre for Research in Experimental Space Science, York University, Toronto, Ontario, Canada, 1972.
25. K. P. HUBER AND G. HERZBERG, "Constants of Diatomic Molecules," Van Nostrand-Reinhold, New York, 1979.
26. T. A. DIXON AND R. C. WOODS, *J. Chem. Phys.* **67,** 3956–3964 (1977).
27. D. A. SKATRUD, F. C. DELUCIA, G. A. BLAKE, AND K. V. L. N. SASTRY, *J. Mol. Spectrosc.* **99,** 35–46 (1983).
28. M. A. JOHNSON, M. L. ALEXANDER, I. HERTEL, AND W. C. LINEBERGER, *Chem. Phys. Lett.* **105,** 374–379 (1984).

29. H. ITO, S. YAMAMOTO, S. SAITO, AND K. KUCHITSU, "46th International Symposium on Molecular Spectroscopy, Columbus, Ohio," June 1991. [Abstract TG8], *Chem. Phys. Lett.*, in press.
30. M. BOGEY, C. DEMUYNCK, AND J. L. DESTOMBES, *Can. J. Phys.* **62,** 1248–1253 (1984).
31. A. J. KOTLAR, R. W. FIELD, J. I. STEINFELD, AND J. A. COXON, *J. Mol. Spectrosc.* **80,** 86–108 (1980).
32. Y. OZAKI, T. NAGATA, K. SUZUKI, T. KONDOW, AND K. KUCHITSU, *Chem. Phys.* **80,** 73–84 (1983); Y. OZAKI, H. ITO, K. SUZUKI, T. KONDOW, AND K. KUCHITSU, *Chem. Phys.* **80,** 85–94 (1983).
33. H. ITO, Y. OZAKI, T. NAGATA, T. KONDOW, AND K. KUCHITSU, *Can. J. Phys.* **62,** 1586–1596 (1984).
34. H. ITO, Y. OZAKI, K. SUZUKI, T. KONDOW, AND K. KUCHITSU, *Chem. Phys. Lett.* **139,** 581–584 (1987).
35. H. ITO, Y. FUKUDA, Y. OZAKI, T. KONDOW, AND K. KUCHITSU, *J. Mol. Spectrosc.* **121,** 84–90 (1987).
36. H. ITO, Y. OZAKI, K. SUZUKI, T. KONDOW, AND K. KUCHITSU, *J. Mol. Spectrosc.* **127,** 143–155, 283–303 (1988).
37. S. P. DAVIS, M. C. ABRAMS, M. L. P. RAO, AND J. W. BRAULT, *J. Opt. Soc. Am. B* **8,** 198–200 (1991).
38. H. ITO, K. SUZUKI, T. KONDOW, AND K. KUCHITSU, *J. Chem. Phys.* **94,** 5353–5359 (1991).
39. C. W. BAUSCHLICHER, JR., S. R. LANGHOFF, AND P. R. TAYLOR, *Astrophys. J.* **332,** 531–538 (1988).
40. N. FURIO, A. ALI, P. J. DAGDIGIAN, AND H.-J. WERNER, *J. Mol. Spectrosc.* **134,** 199–213 (1989).
41. P. J. KNOWLES, H.-J. WERNER, P. J. HAY, AND D. C. CARTWRIGHT, *J. Chem. Phys.* **89,** 7334–7343 (1988).
42. P. G. CARRICK, C. R. BRAZIER, P. F. BERNATH, AND P. G. ENGELKING, *J. Am. Chem. Soc.* **109,** 5100–5102 (1987).
43. N. OLIPHANT, A. LEE, P. F. BERNATH, AND C. R. BRAZIER, *J. Chem. Phys.* **92,** 2244–2247 (1990).
44. P. C. ENGELKING, *Rev. Sci. Instrum.* **57,** 2274–2277 (1986).
45. P. F. BERNATH, C. R. BRAZIER, T. OLSEN, R. HAILEY, W. T. M. L. FERNANDO, C. WOODS, AND J. L. HARDWICK, *J. Mol. Spectrosc.* **147,** 16–26 (1991).
46. E. C. RICHARD, D. J. DONALDSON, AND V. VAIDA, *Chem. Phys. Lett.* **157,** 295–299 (1989).
47. B. D. REHFUSS, M. H. SUH, T. A. MILLER, AND V. E. BONDYBEY, "46th International Symposium on Molecular Spectroscopy, Columbus, Ohio," June 1991. [Abstract TG7], *J. Mol. Spectrosc.* **151,** 437–438 (1992).
48. D. COSSART, C. COSSART-MAGOS, G. GANDARA, AND J. M. ROBBE, *J. Mol. Spectrosc.* **109,** 166–185 (1985).
49. G. NORLEN, *Phys. Scr.* **8,** 249–268 (1973).
50. G. HERZBERG, "Spectra of Diatomic Molecules," Van Nostrand–Reinhold, New York, 1950.
51. J. M. BROWN, E. A. COLBOURN, J. K. G. WATSON, AND F. D. WAYNE, *J. Mol. Spectrosc.* **74,** 425–436 (1979).
52. M. DOUAY, S. A. ROGERS, AND P. F. BERNATH, *Mol. Phys.* **64,** 425–436 (1988).